4374 J. Am. Chem. Soc. 1984, 106, 4374-4378

3,5,11,13-Tetraazacycl[3.3.3]azine: Theoretical (ab Initio) and Experimental (X-ray and Ultraviolet Photoelectron Spectroscopy) Studies of the Electronic Structure

J. P. Boutique,[*,†,§] **J. J. Verbist,**[†] **J. G. Fripiat,**[‡] **J. Delhalle,**[‡] **G. Pfister-Guillouzo,**[⊥] **and G. J. Ashwell**[∥]

Contribution from the Laboratoire de Spectroscopie Électronique and Laboratoire de Chimie Théorique Appliquée, Facultés Universitaires Notre-Dame de la Paix, B-5000 Namur, Belgium, Laboratoire de Physico-Chimie Moléculaire—CNRS ERA 895, Université de Pau, F-64016 Pau, France, and the Department of Chemistry, Sheffield City Polytechnic, Sheffield S1 1WB, United Kingdom. *Received December 27, 1983*

Abstract: Electronic structure and bonding of 3,5,11,13-tetraazacycl[3.3.3]azine are studied by theoretical calculations and photoelectron spectroscopy. Both approaches present indications as to the more positive nature of the central nitrogen atom and of the involvement of its lone pair in the delocalization pattern. The nature and sequence of the highest occupied levels are discussed.

Polycyclic systems containing three rings fused around a common central atom have been the subject of thorough experimental and theoretical studies for many years. The pure hydrocarbon compound representative of the series of interest herein is the phenalenylium radical (Figure 1a), which has been shown to be aromatic and relatively stable, though, even at low temperatures, it dimerizes in solution.[1,2] With the goal of preparing new types of conducting charge-transfer complexes, attempts have been made to increase the stability of the radical by incorporating disulfide bridges in the structure;[3] so far these efforts have met with relative success.

Replacing the central carbon atom by nitrogen leads to the more favorable closed shell situation, due to the extra electron, and is another way to stabilize further the system. This approach has contributed to the development of a new family of compounds: the cyclazines. Heterocycles characterized by 5- or 6-membered rings condensed around a central nitrogen have already drawn considerable interest, owing to their many-sided aromatic character.[4-22]

While cycl[3.2.2]azines (Figure 1b) exhibit a strong aromatic character, cycl[3.3.3]azines (Figure 1c) do not. This is in agreement with predictions from semiempirical MO calculations[8] and is confirmed by ^{1}H NMR[9] and their chemical instability (e.g., to air exposure, oxidation, and reduction[21]). However, replacing several of the peripheral carbons by nitrogens in cycl[3.3.3]azines, e.g., Figures 1d,e, seems to restore aromaticity,[10-20] even though the formal number of π-electrons actually involved in the delocalization scheme remains the same. Several compounds of this type have already been prepared, such as the 3,5,11-tri-,[11] 3,5,9,11-tetra-,[14] 3,5,11,13-tetra-,[10] 3,5,7,11-tetra-[16]; and 3,5,13-triazocycl[3.3.3]azines,[19] which, incidently, give some hope for application in the area of pharmacology.[11]

In spite of the unusual behavior of these compounds, few theoretical calculations—all at a semiempirical level—and no photoemission data have been reported to date. In an attempt to provide some of the missing information, results of ab initio calculations on 3,5,11,13-tetraazacycl[3.3.3]azine (I), and X-ray and ultraviolet photoelectron spectroscopy (XPS and UV PES, respectively) data on I and its 4,12-dimethyl derivative (II) are discussed. Emphasis in the analysis is put on the involvement of the central nitrogen lone pair in the π delocalization, and on the nature and energy of the highest occupied molecular orbitals.

Methodology

A. Theoretical Calculations. Restricted Hartree–Fock–Roothaan (LCAO–MO–SCF) results on I have been obtained with STO-3G minimal basis set,[23] using the GAUSSIAN 80 series of programs.[24] Structural parameters from X-ray diffraction measurements have been used in a slightly modified form to adjust the geometry to C_{2v} point group symmetry. All integrals larger than 10^{-6} were retained, and the convergence threshold on density matrix elements was smaller than 5×10^{-5}. Correlation of the photoemission and calculated data are based on the assumed validity of Koopmans' theorem.[25] Calculations reported here were carried out on the DEC 2060 computer of the Facultés Universitaires de Namur.

B. Experimental Procedure. Both compounds, I and II, were prepared according to the methods given in the literature.[10]

[†] Laboratoire de Spectroscopie Electronique, Facultés Universitaires Notre-Dame de la Paix.

[‡] Laboratoire de Chimie Théorique Appliquée, Facultés Universitaires Notre-Dame de la Paix.

[§] Research assistant of the NFSR, Belgium.

[⊥] Université de Pau.

[∥] Sheffield City Polytechnic.

(1) Reid, D. H. *Tetrahedron* **1958**, *3*, 339.

(2) Gerson, F. *Helv. Chim. Acta* **1966**, *49*, 1463. Gerson, F.; Heilbronner, E.; Reddock, H. A.; Paskovich, D. A.; Das, N. C. *Ibid.* **1967**, *50*, 813.

(3) Haddon, R. C.; Wudl, F.; Kaplan, M. L.; Marshall, J. H.; Bramwell, F. B. *J. Chem. Soc., Chem. Commun.* **1978**, 429. Haddon, R. C.; Wudl, F.; Kaplan, M. L.; Marshall, J. H.; Cais, R. E.; Bramwell, F. B. *J. Am. Chem. Soc.* **1978**, *100*, 7629.

(4) Windgassen, R. J.; Saunders, W. H., Boekelheide, V. *J. Am. Chem. Soc.* **1959**, *81*, 1459.

(5) Boekelheide, V.; Small, T. *J. Am. Chem. Soc.* **1960**, *83*, 462.

(6) Gerson, F.; Heilbronner, E.; Joop, N.; Zimmerman, H. *Helv. Chim. Acta* **1963**, *46*, 1940.

(7) Boekelheide, V.; Gerson, F.; Heilbronner, E.; Meuche, D. *Helv. Chim. Acta* **1963**, *46*, 1951.

(8) Dewar, M. J. S.; Trinajstic, N. *J. Chem. Soc. A* **1969**, 1754.

(9) Farquhar, D.; Leaver, D. *J. Chem. Soc. Chem. Commun.* **1969**, 24.

(10) Shaw, J. T.; Westler, W. M.; Stefanko, B. D. *J. Chem. Soc., Chem. Commun.* **1972**, 1070. Shaw, J. T.; Balik, C. M.; Holodmak, J. L.; Prem, S. *J. Heterocycl. Chem.* **1976**, *13*, 127.

(11) Ceder, O; Andersson, J. E. *Acta Chem. Scand.* **1972**, *26*, 596.

(12) Ceder, O.; Andersson, J. E. *Acta Chem. Scand.* **1972**, *26*, 611.

(13) Ceder, O.; Andersson, J. E.; Johansson, L. E. *Acta Chem. Scand.* **1972**, *26*, 624.

(14) Ceder, O.; Witte, J. F. *Acta Chem. Scand.* **1972**, *26*, 635.

(15) Ceder, O.; Rosen, K. *Acta Chem. Scand.* **1973**, *27*, 359.

(16) Ceder, O.; Rosen, K. *Acta Chem. Scand.* **1973**, *27*, 2421.

(17) Ceder, O.; Vernmark, K., *Acta Chem. Scand.* **1973**, *27*, 3259.

(18) Ceder, O.; Samuelsson, M. L. *Acta Chem. Scand.* **1973**, *27*, 3264.

(19) Ceder, O., Vernmark, K. *Acta Chem. Scand.* B **1977**, *B31*, 235.

(20) Ceder, O.; Vernmark, K. *Acta Chem. Scand. B* **1977**, *B31*, 239.

(21) Farquhar, D.; Gough, T. T.; Leaver, D. *J. Chem. Soc., Perkin Trans 1* **1976**, 341.

(22) Lindqvist, O.; Ljungström, E.; Ceder, O. *Acta Crystallogr. Sect. B* **1978**, *B34*, 1667.

(23) Hehre, W. J.; Ditchfield, R.; Stewart, R. F.; Pople, J. A. *J. Chem. Phys.* **1970**, *52*, 2769.

(24) Binkley, J. S.; Whiteside, R. A.; Krishnan, R.; Seeger, R.; Defrees, D. J.; Schlegel, H. B.; Topiol, S.; Kahn, L. R.; Pople, J. A. *QCPE* **1981**, *13*, 406.

(25) Koopmans, T. A. *Physica (Amsterdam)* **1933**, *1*, 104.

0002-7863/84/1506-4374$01.50/0

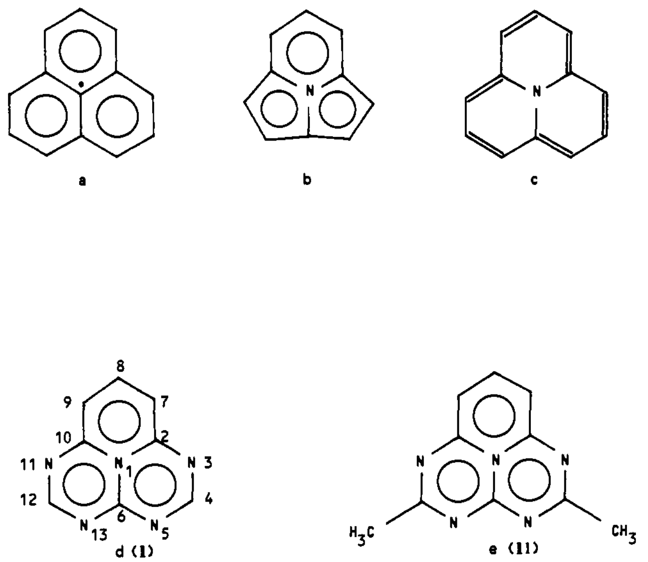

Figure 1. Schematic molecular structures of (a) the phenalenylium radical, (b) cycl[3.2.2]azine, (c) cycl[3.3.3]azine, (d) 3,5,11,13-tetraazacycl[3.3.3]azine (I), and (e) 4,12-dimethyl 3,5,11,13-tetraazacycl[3.3.3]azine (II).

For XPS measurements, samples were crushed and then pressed in pellet form on a gold substrate. XPS spectra were recorded at room temperature on a Hewlett-Packard 5950A spectrometer, using the monochromatized Al $K\alpha_{1,2}$ radiation (1486.6 eV) as incident source. The pressure in the analysis chamber was kept lower than 4×10^{-9} torr. The flood-gum technique has been used to neutralize charging effects at the surface. Wide-energy scan spectra revealed negligible oxygen contamination in I as indicated by the occurrence of a very weak O1s line; nothing similar could even be detected in II. Calibration was achieved by fixing the C1s line related to the quasi-neutral C_7 and C_9 atoms at 284.4 eV, a typical binding energy found in graphite,[26] acenes,[27] and poly(*p*-phenyls).[28]

He I UV PES spectra were recorded on a Helectros"078" spectrometer. The $Ar3p_{3/2}$ (15.76 eV), $Ar3p_{1/2}$ (15.93 eV), $Xe5p_{3/2}$ (12.13 eV), and $Xe5p_{1/2}$ (13.43 eV) lines were used for calibration. The average precision on ionization potentials is estimated to 0.05 eV.

Theoretical Results

Though very controversial,[29,30] the aromaticity concept is nonetheless widely used in the discussion of bonding in ring systems involving conjugated π bonds. Characterization of ground-state aromaticity is based on physical properties such as geometry (bond length, planarity, etc.), NMR chemical shifts, resonance, and stabilization energy. Atomic and overlap populations from theoretical calculations also constitute valuable indices by which to assess the aromatic status of a molecule. Hereafter such theoretical quantities are analyzed to obtain additional insight into the delocalization pattern taking place at the periphery of system I as well as on the nature of the highest occupied molecular orbitals.

Table I collects the values of total energy, gross atomic charges, and overlap populations. Since no geometry optimization has been carried out in this work, total energy is given here for indicative purposes only.

Gross atomic charges on the carbon and nitrogen atoms follow expected trends. The amount of electron charge transferred from the carbons to the adjacent and more electronegative nitrogens is in direct relation to the number of the latter. Conversely, the nitrogens are all found negative, with an average excess electron charge of 0.31 except for the central N_1, for which this excess, 0.23, is less marked. To further analyze this difference and its implications on the bonding, the gross atomic charges have also been sorted by their 2s, $2p_x + 2p_y$, σ ($=2s + 2p_x + 2p_y$), and $\pi(2p_z)$ contributions (Table I). Notice that, as in pyrrole, N_1 formally contributes two electrons to the π system while each peripheral nitrogen (N_3, N_5, N_{11}, N_{13}), analogous to the one in pyridine, brings one electron. Furthermore, N_1 acts as a σ acceptor ($q_\sigma = 3.77$) and π donor ($q_\pi = 1.47$), contrary to the other nitrogens which are σ and π acceptors ($q_\sigma \simeq 4.06$, $q_\pi = 1.25$).

Table I. Theoretical Calculations on 3,5,11,13-Tetraazacycl[3.3.3]azine (I): Total Energy, Electronic Charges, and Mulliken Overlap Populations

	electronic charges[b]				
	q_{total}	q_{2s}	$q_{2p_x+2p_y}$	q_σ	q_π
N_1	7.232	1.459	2.313	3.772	1.465 (1.464)[a]
$C_{2,10}$	5.741	1.079	1.765	2.844	0.904
$N_{3,11}$	7.310	1.621	2.454	4.075	1.239
$C_{4,12}$	5.829	1.104	1.875	2.979	0.857
$N_{5,13}$	7.305	1.624	2.428	4.052	1.256
C_6	5.659	1.055	1.702	2.757	0.909
$C_{7,9}$	6.140	1.078	1.933	3.011	1.136
C_8	5.992	1.144	2.014	3.158	0.841

total energy, au	Mulliken overlap population, $2p_z$–$2p_z$			
−570.742 42 (−570.742 15)[a]	N_1–C_2	0.062 (0.061)[a]	N_5–C_6	0.089
	C_2–N_3	0.069	C_6–N_1	0.050
	N_3–C_4	0.117	C_2–C_7	0.103
	C_4–C_5	0.090	C_7–C_8	0.107

[a] These parameters refer to the nonplanar conformation, where the N_1 nitrogen atom is distant of 0.033 Å from the plane of the other non-hydrogen atoms. Both planar and nonplanar conformations are quite similar: the Mulliken populations indices are nearly identical, and the total energy difference is unsignificant. [b] Atoms are labeled as mentioned in Figure 1.

Relative values of π-overlap populations on the various bonds are often involved in the assignation of an aromatic character to a molecule. Here it can be noticed that, except for C_2–N_3 and its symmetrical C_{10}–N_{11}, π-overlap populations on peripheral bonds are quite similar, with an average and relatively high value, 0.096, while the N_1–C_6, N_1–C_2 and N_1–C_{10} central bonds present a smaller average value, 0.054. It should be stressed, however, that, contrary to the other nitrogens, N_1 is involved in three bonds. Since it is known from X-ray diffraction that N_1 is located 0.033 Å out of the plane defined by the other atoms, we have performed an additional calculation with N_1 in this situation to assess the influence of nonplanarity on the π-overlap populations of N_1–C_2. It turns out that the effect is negligible, as observed from the values in parentheses in Table I.

The π-overlap data suggest that a conclusion[23] that the observed average distance, 1.40 Å, from N_1 to its neighboring carbons is indicative of no interaction between central and peripheral electrons is obviously too strong. Even if per bond the N_1–C overlap populations are smaller than on the molecular perimeter, it is nonetheless significant, and likewise a picture of a bridged [12] annulenic system is exaggerated.

A proper description of the role of peripheral nitrogens in restoring the aromatic character when going from cycl[3.3.3]azine (Figure 1c) to I or 1,3,4,6-tetraazacycl[3.3.3]azine would require systematic calculations on various terms of the *n*-azacycl[3.3.3]azine series where geometry optimization would be necessary. It is nonetheless tempting to take the similar values of π-overlap population on C_2–C_7, C_7–C_8, C_2–N_3, N_3–C_4, C_4–N_5, N_5–C_6, and their equivalents as clues of aromatic character, driven by a favorable intramolecular combination of π-electron-donating (N_1), and π-electron-accepting (peripheral nitrogens) systems. Through this, enough electron charge is pumped into the "annulenic" framework, so that is partly recovers an aromatic status.

We now turn to the analysis of the higher occupied one-electron levels to be used later in the interpretation of photoelectron

---

(26) Wertheim, G. K.; Van Attekum, P. M. T. M.; Basu, S. *Solid State Commun.* **1980**, *33*, 1127.

(27) Riga, J.; Pireaux, J. J.; Caudano, R.; Verbist, J. J. *Phys. Scr.* **1977**, *16*, 346.

(28) Riga, J.; Pireaux, J. J.; Boutique, J. P.; Caudano, R.; Verbist, J. J.; Gobillon, Y. *Synth. Met.* **1981**, *4*, 99.

(29) "Aromaticity, pseudo-aromaticity, anti-atomaticity"; Bergmann, E. D., Pullman, Eds.; Jerusalem Academic Press: Jerusalem, 1981.

(30) Labarre, J. F.; Crasnier, F.; *Top. Curr. Chem.* **1971**, *24*, 33.

Table II. Monoelectronic Energy Levels of 3,5,11,13-Tetraazacycl[3.3.3]azine (I) (eV)

level (C_{2v})	character	energy (no. of levels)	level (C_{2v})	character	energy (no. of levels)
N_1s	N_1	−422.83	$7a_1$	sσ	20.55
	$N_{3,11}$	417.43 (2)	$8a_1$	pσ	19.79
	$N_{5,13}$	417.18 (2)	$6b_2$	pσ	19.36
C_1s	C_6	305.34	$9a_1$	pσ	18.05
	$C_{2,10}$	304.86 (2)	$1b_1$	pπ	17.86
	$C_{4,12}$	303.56 (2)	$7b_2$	pσ	16.88
	C_8	302.45	$10a_1$	pσ	16.82
	$C_{7,9}$	300.94 (2)	$8b_2$	pσ	15.36
			$9b_2$	pσ	14.63
$1a_1$	sσ	37.62	$11a_1$	pσ	14.51
$1b_2$	sσ	34.58	$1a_2$	pπ	14.00
$2a_1$	sσ	33.52	$2b_1$	pπ	13.67
$3a_1$	sσ	32.17	$3b_1$	pπ	11.66
$2b_2$	sσ	30.72	$12a_1$	pσ	11.50
$4a_1$	sσ	29.91	$10b_2$	pσ	11.09
$3b_2$	sσ	27.52	$4b_1$	pπ	10.24
$5a_1$	sσ	24.50	$2a_2$	pπ	9.97
$6a_1$	sσ	24.40	$11b_2$	n_N	9.28
$4b_2$	sσ	24.16	$13a_1$	n_N	9.10
$5b_2$	sσ	20.66	$3a_2$ (HOMO)	pπ	−5.46
			$5b_1$ (LUMO)	pπ	+3.35

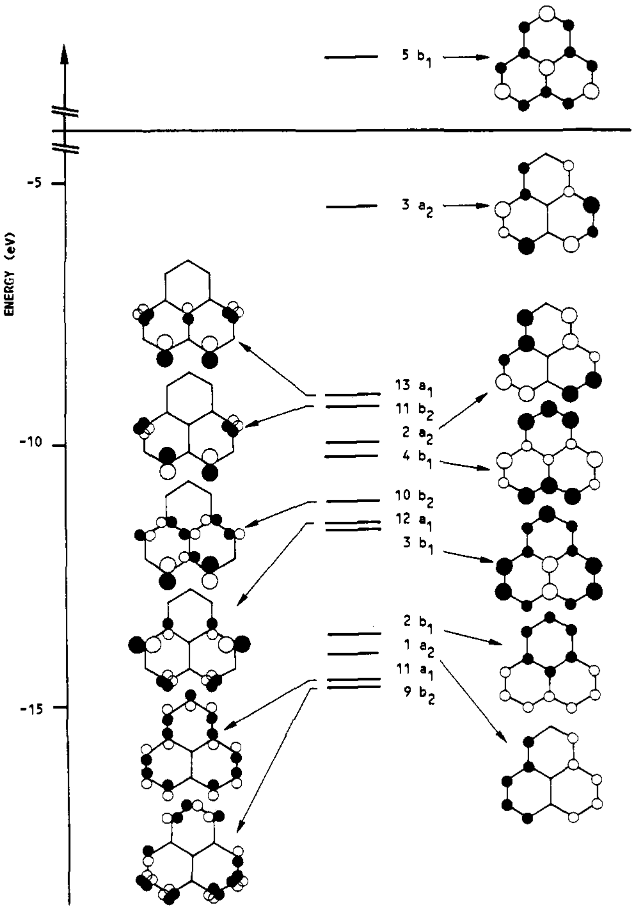

Figure 2. Schematic diagram of the highest occupied molecular orbitals.

spectroscopic measurements. Energies and symmetry labels of the one-electron states are listed in Table II, while the dominant atomic functions entering the LCAO representation of the most relevant MO's are sketched in Figure 2.

The HOMO ($3a_2$) is of π nature, and predicted to be at a substantially higher value on the energy scale (−5.46 eV) than the next occupied molecular orbitals. Major contributions come from $2p_z$ atomic functions on the peripheral nitrogens and on the C_7 and C_9 atoms; the σ_v passing through C_8–C_6 and perpendicular to the molecular framework is also a nodal plane for the HOMO. As a whole, the HOMO develops a slight quinoid form, with the largest π overlaps on C_3–C_4 and C_2–C_7 bonds parallel to the C_2 axis.

The HOMO is followed by a group of seven one-electron states in the energy range of −9.10 to −11.66 eV. The two highest energy states ($13a_1$ and $11b_2$) are of σ type; they relate to the lone pairs of the peripheral nitrogens. The next two MO's ($2a_2$ and $4b_1$) of π type are respectively antisymmetric and symmetric combinations of the $2p_z$ functions with respect to the σ_v plane. The $10b_2$ level (−11.09 eV) is the first MO clearly related to the σ bonding; it represents a σ bonding situation for the N_3–C_2–N_1–C_{10}–N_{11} sequence of atoms on the one hand, and exhibits nitrogen lone-pair character due to N_5 and N_{13}. The last two MO's of this group are $\sigma 12a_1$, another nitrogen lone pair related orbital, and $\pi 3b_1$, which accounts for the π-electron delocalization on the annulene part of the molecule. At somewhat lower energies are found first the $\pi 2b_1$ and $\pi 1a_2$ and then the $11a_1$ and $9b_2$ levels, which describe the σ_{N-C} and σ_{C-C} bonds.

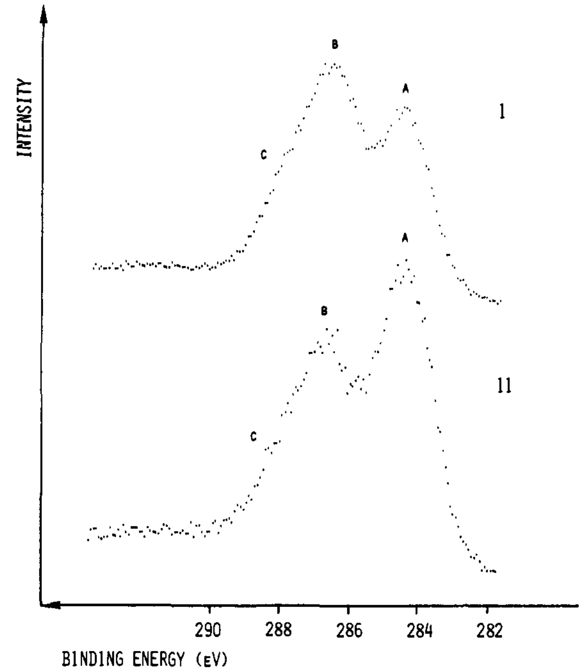

Figure 3. C1s core level spectra of 3,5,11,13-tetraazacycl[3.3.3]azine (I) and of its 4,12-dimethyl derivative (II).

Table III. 3,5,11,13-Tetraazacycl[3.3.3]azine (I) and Its 4,12-Dimethyl Derivative (II): N1s and C1s Core Level Binding Energies (eV)

	I	II
C1s	A: 284.4	A: 284.4
	B: 286.5	B: 286.6
	C: 287.9	C: 288.1
N1s	A: 398.3	A: 398.3
	B: 401.3	B: 401.3

Photoelectron Spectroscopy Results

A. XPS. Position, intensity, and shift of the core levels obtained from X-ray photoelectron spectroscopy provide suitable information to verify theoretical results on electron density distributions in the molecule. In Figure 3 and 4 are respectively reproduced the experimental C1s and N1s core level spectra of I and II. The binding energies are listed in Table III. No shake-up features have been observed.

C1s lines can be interpreted by reference to the calculated MO energies. Peak A is assigned to atoms C_7 and C_9. Under peak B are comprised contributions from C_8, C_2, C_4, C_{10}, and C_{12}, while the shoulder denoted by C is likely due to the strongly positive C_6 atom which is surrounded by three nitrogens. As expected,

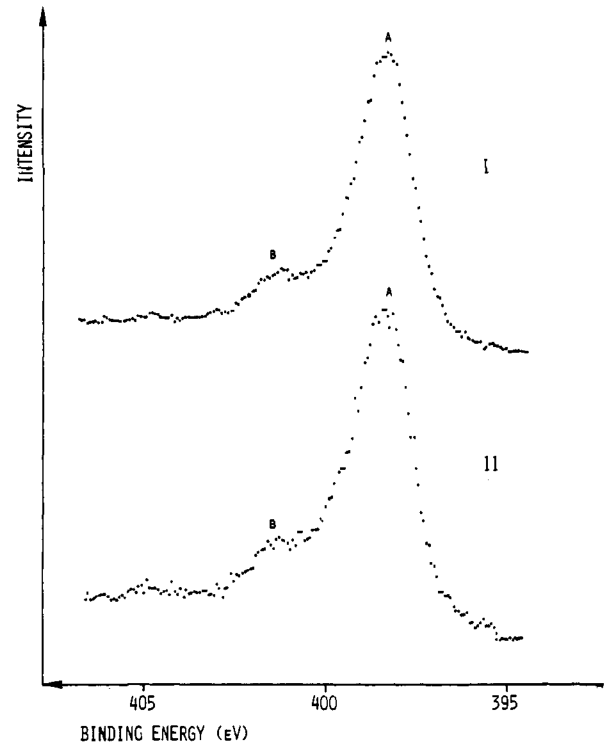

Figure 4. N1s core level spectra of 3,5,11,13-tetraazacycl[3.3.3]azine (I) and of its 4,12-dimethyl derivative (II).

Table IV. Vertical Ionization Energies (eV) of 3,5,11,13-Tetraazacycl[3.3.3]azine (I) and 4,12-Dimethyl Derivative (II)

	I	II
IP_1	8.00	7.70
IP_2	9.80	9.45
IP_3	10.45	10.10–10.35
IP_4	11.05–11.30	10.90
IP_5	11.60	11.20
IP_6	12.05	11.70
IP_7	13.30–13.85	12.60
IP_8	14.20	12.90
IP_9	15.15	13.65
IP_{10}	15.75	15.70

the methyl C1s lines in II appear at nearly the same energy as contributions from C_7 and C_9, and, therefore, belong to peak A.

N1s core level spectra (Figure 4) show two lines separated by an energy difference of 3.0 eV and occurring in a 1:4 intensity ratio, with the lowest intensity peak located at the high binding energy side. This peak is attributed to the central nitrogen, N_1, and constitutes experimental evidence of this being less negative than the others.

B. UV PES. Due to better resolution, UV PES provides a more suitable approach than XPS to the study of the highest occupied levels. Figures 5 and 6 display the gas-phase UV PES spectra of I and II. The main reason for studying in this work the dimethyl derivative, II, is to use the substituents to reveal features in the electronic structure by inducing selective shifts in the levels. Values of experimental ionization potentials (IP_i's) are listed in Table IV. IP_1, the first ionization potential, is assigned to the HOMO $\pi 3a_2$ and, as predicted by calculations, is well separated from the neighboring levels. It should be noticed that under methyl substitution the HOMO in II is shifted by 0.3 eV toward the lower energy values. Such a displacement is significant and results from the substitution of a hydrogen by an electron-donating group ($-CH_3$) at the sensitive electron-deficient sites, C_4 and C_{12}.

In the framework of the frozen orbital approximation,[25] the $\sigma 13a_1$ and $11b_2$ levels are assigned to IP_2. This attribution is likely to be correct, even if final-state effects are nonnegligible. Indeed nitrogen lone-pair levels should remain more destabilized than the deeper π levels[31] even though minimal basis set does not properly account for polarization effects.

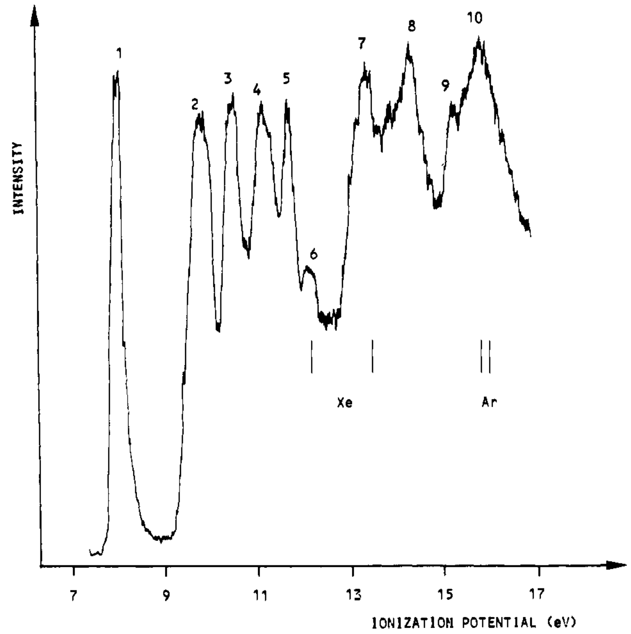

Figure 5. He I UV PES spectrum of 3,5,11,13-tetraazacycl[3.3.3]azine (I).

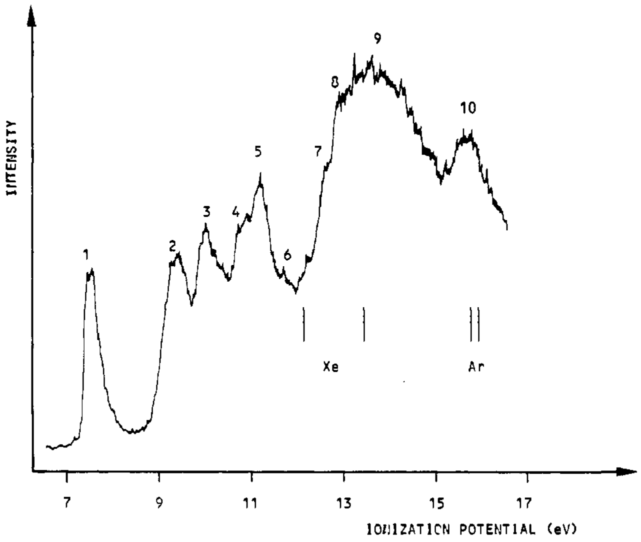

Figure 6. He I UV PES spectrum of 4,12-dimethyl 3,5,11,13-tetraazacycl[3.3.3]azine (II).

IP_3 likely contains the $\pi 2a_2$ and $4b_1$ MO's, which are sufficiently distinct from the following ones, not to be confused with or preceded by them. Dimethylation would shift the $2a_2$ orbital to the lower IP's side much more than the $4b_1$ MO, considering the different electronic density on the substitution site. This is actually observed from the title compound to the dimethylated derivative; the $2a_2$ MO is shifted 0.35 eV from 10.45 to 10.10 eV, while the $4b_1$ MO is much less affected, shifting from 10.45 to 10.35 eV.

We associate IP_4 with the $\sigma 10b_2$ orbital, describing the peripheral nitrogen lone pairs, with some σ_{CN} bonding character, and IP_5 and IP_6 with orbitals $\pi 3b_1$ and $\sigma 12a_1$. Dimethylation strongly affects the $\pi 3b_1$ orbital by shifting it from 11.60 to 11.20 eV, very close to the $\sigma 10b_2$ (IP_4) orbital, as this orbital is only displaced by ~0.15 eV ($10b_2$ presents nodes on the substitution sites). The position of the $\sigma 12a_1$ MO is less obvious, but we think that it is localized near IP_5 and partially appears in IP_6.

---

(31) Malrieu, J. P. Comptes Rendus de la Journée sur la Spectroscopie Photoelectronique (rayonnement U.V.), Paris, 1978.

J. Am. Chem. Soc. **1984**, *106*, 4378–4380

The gap between 11.7 and 13.6 eV on the calculated energy scale is visible on the spectra between 12.0 and 12.5 eV. Then the $\pi 2b_1$ and $1a_2$ MO's arise, followed by the σ_{C-N} and σ_{C-C} orbitals. The differences between the two spectra around 13.7 eV are due to the presence of additional σ_{C-C} and σ_{C-H} orbitals in the dimethylated compound.

Concluding Remarks

Theoretical ab initio calculations shed some light on the molecular structure of 3,5,11,13-tetraazacycl[3.3.3]azine: the Mulliken population analysis indicates a nonnegligible involvement of the central nitrogen lone pair in the delocalization pattern. XPS results on C1s and N1s core levels confirm this assumption, the central nitrogen appearing much less negative than the others. The UV PES spectra may be successfully interpreted on the basis of Koopmans' theorem and correlated with the calculated molecular orbital energies.

The usefulness of the joint study of the theoretical and XPS, UV PES experimental results is thus firmly established in the field on aromatic nitrogen-containing compounds.

Acknowledgment. Helpful discussions with Dr J. Riga (Namur) and Drs. D. Gonbeau and C. Guimon (Pau) are greatly acknowledged. We thank F. Gracian (Pau) and Ph. Henrot (Namur) for technical assistance. One of us (J.P.B.) is grateful to the F.N.R.S. (Belgium) and to the Belgian–French exchange program with the C.N.R.S (France) for assistance during his stay at the University of Pau.

Registry No. I, 38713-73-4; II, 38713-72-3.

Semiempirical Calculation of Diamagnetic Susceptibilities of Alkyl β-Aminovinyl Ketones

R. R. Gupta,* Ratan Swaroop, M. Kumar, and Kishan

Contribution from the Department of Chemistry, University of Rajasthan, Jaipur-302004, India.
Received January 11, 1984

Abstract: Diamagnetic susceptibilities of alkyl β-aminovinyl ketones have been calculated theoretically by different theoretical approaches. The wave-mechanical approach, however, gives due consideration to the contributions of all types of electrons, but still the agreement between experimental and theoretical values is not satisfactory. The semiempirical approach, in which diamagnetic susceptibility is considered to be contributed by atoms, bonds, and bond–bond interactions, provided excellent results of diamagnetic susceptibility irrespective of the existing different structural environments. The divergency between experimental and theoretical values of diamagnetic susceptibility is less than 1%. Such an excellent agreement is due to the fact that all the existing structural factors have been duly accounted for in the form of parameters.

Diamagnetic susceptibility has been fascinating to the scientists since it has proved its unique importance by giving structural information on resolving various existing structural controversies in structural chemistry. But the diamagnetic studies, in view of their relationship with the structure, require theoretical estimations of diamagnetic susceptibilities for analyzing different existing structural environments, since such structural environments affect considerably the molecular diamagnetism. Although a number of methods,[1-5] based on either the atomic susceptibility concept or the bond susceptibility concept, have been developed to calculate diamagnetic susceptibilities of organic compounds but could not provide satisfactory results of diamagnetic susceptibility even for simple organic compounds. It is, therefore, considered interesting to develop a semiempirical approach to calculate diamagnetic susceptibilities of the alkyl β-aminovinyl ketones analogous to that reported for the simple organic and organometallic compounds,[6-8] since alkyl β-aminovinyl ketones form an interesting and exciting series of organic compounds, from a structural point of view, because of the presence of a carbonyl group in conjugation with doubly bonded carbon atom and due to the presence of a nitrogen atom having a lone pair of electrons. The results obtained by theoretical approaches, other than the semiempirical approach, have also been analyzed in the light of structural factors prevailing in the alkyl β-aminovinyl ketones and contributing considerably to the molecular diamagnetism.

Diamagnetic susceptibilities of the alkyl β-aminovinyl ketones have been calculated theoretically by the Pascal, Pacault, and Hoarau method, based on the atomic susceptibility concept, and the wave–mechanical method, based on the bond susceptibility concept, in order to analyze different existing structural environments and to correlate these structural environments with the theoretical results. The Pascal, Pacault, and Hoarau method considers the contributions of atoms and the correction factors of the methyl group. The wave–mechanical approach has been applied to calculate diamagnetic susceptibilities by using the contributions of (i) inner-shell electrons of each atom present, (ii) bonding electrons in each bond, (iii) a nonbonding lone pair of electrons present in the outer shell, and (iv) π-electrons in the form of the following expression:

$$\chi_M = \sum\chi_{ISE} + \sum\chi_{BE} + \sum\chi_{NBE} + \sum\chi_{\pi\text{-electrons}}$$

The results of diamagnetic susceptibility of the alkyl β-aminovinyl ketones, obtained by the Pascal, Pacault, and Hoarau method as well as the wave–mechanical approach, are summarized in Table I.

A critical examination of the theoretical results of diamagnetic susceptibility of the alkyl β-aminovinyl ketones, calculated by the

---

(1) Pascal, P. *Ann. Chim. Phys.* **1910**, *19*, 5.

(2) Yang, Y. *J. Chem. Phys.* **1948**, *16*, 865.

(3) Pascal, P.; Gallais, F.; Labarre, J. F. *C. R. Hebd. Seances Acad. Sci.* **1951**, *252*, 2624.

(4) Pascal, P.; Pacault, A.; Hoarau, J. *C. R. Hebd. Seances Acad. Sci.* **1951**, *233*, 1078.

(5) (a) Baudet, J.; Tillieu, J.; Guy, J. *C. R. Hebd. Seances Acad. Sci.* **1957**, *244*, 2920. (b) Baudet, J. *J. Chim. Phys.* **1961**, *58*, 228. (c) Baudet, J.; Guy, J.; Tillieu, J. *J. Phys. Radium* **1960**, *21*, 600.

(6) (a) Hameka, H. F. *J. Chem. Phys.* **1961**, *34*, 1996. (b) O'Sullivan, P. S.; Hameka, H. F. *J. Am. Chem. Soc.* **1970**, *92*, 25; 1821.

(7) Burnham, A. K.; Lee, J.; Schmalz, T. G.; Beak, P.; Flygare, W. H. *J. Am. Chem. Soc.* **1977**, *99*, 1836.

(8) (a) Mital, R. L.; Gupta, R. R. *J. Am. Chem. Soc.* **1969**, *91*, 4664. (b) Gupta, R. R.; Kumar, M.; Ojha, K. G. *J. Chem. Phys.* **1981**, *75*, 4173; **1982**, *76*, 1173; 5182. (c) Gupta, R. R.; Kumar, M. *Chem. Phys. Lett.* **1983**, *100*, 297.

0002-7863/84/1506-4378$01.50/0